Astron. Astrophys. 285, 621–630 (1994)

ASTRONOMY AND ASTROPHYSICS

The soft X-ray/microwave ratio of solar and stellar flares and coronae

A.O. Benz[1] **and M. Güdel**[2]

[1] Institute of Astronomy, ETH-Zentrum, CH-8092 Zürich, Switzerland
[2] Joint Institute for Laboratory Astrophysics, University of Colorado and National Institute of Standards and Technology, Boulder, CO 80309-0440, USA

Received 21 July 1993 / Accepted 9 October 1993

Abstract. We have carried out plasma diagnostics of solar flares using soft X-ray (SXR) and simultaneous microwave observations and have compared the ratio of X-ray to microwave luminosities of solar flares with various active late-type stars available in the published literature. Both the SXR low-level ('quiescent') emission from stellar coronae and the flaring emission from the Sun and stars are generally interpreted as thermal radiations of coronal plasmas. On the other hand, the microwave emission of stars and solar flares is generally attributed to an extremely hot or nonthermal population of electrons. Solar flare SXR are conventionally measured in a narrower and harder passband than the stellar sources. Observations of the GOES-2 satellite in two energy channels have been used to estimate the luminosity of solar flares as it would appear in the ROSAT satellite passband.

The solar and stellar flare luminosities fit well at the lower end of the active stellar coronae. The flare SXR/microwave ratio is similar to the ratio for stellar coronae. The average ratio follows a power-law relation $L_X \propto L_R^{0.73\pm0.03}$ over 10 orders of magnitude from solar microflares to RS CVn and FK Com-type coronae. Dwarf Me and Ke stars, and RS CVn stars are also compatible with a linear SXR/microwave relation, but the ratio is slightly different for each type of star. Considering the differences between solar flares, stellar flares and the various active stellar coronae, the similarity of the SXR/microwave ratios is surprising. It suggests that the energetic electrons in low-level stellar coronae observed in microwaves are related in a similar way to the coronal thermal plasma as flare electrons to the flare thermal plasma, and, consequently, that the heating mechanism of active stellar coronae is a flare-like process.

Key words: stars: activity – Sun: flares – radio continuum: stars – X-rays: stars – stars: coronae – stars: flare

Send offprint requests to: A.O. Benz

1. Introduction

The existence of an extremely hot corona on the Sun and many other late-type stars is an old, but persisting riddle of astronomy. One of several theories for coronal heating postulates that frequent flares, believed to be the result of magnetic energy dissipation, release the required energy. Previously, this suggestion has been based on a correlation between the average energy release rate observed in optical U-band flares and the low-level (or 'quiescent', i.e. apparently non-flaring) soft X-ray (SXR) luminosity in dMe stars (Doyle & Butler 1985; Whitehouse 1985; Skumanich 1985). However, a relationship between low-level and flaring activity is not unexpected if both originate from magnetic energy built up by the same dynamo process in the stellar interior. Furthermore, sensitive stellar SXR observations (Ambruster et al. 1987) have failed to exhibit continuous low-amplitude flaring activity proposed to provide the energy for the quasi-steady low-level emissions.

Some coronae of active stars of late spectral type are detected microwave sources. The microwave spectral luminosity, L_R, has been found to be roughly proportional to the SXR luminosity, L_X, in RS CVn binaries (Drake et al. 1989, 1992; Dempsey et al. 1993), in dK stars (Güdel 1992), and dMe stars (Güdel et al. 1993a, including strictly simultaneous observations in both wavelength regimes; see also Bookbinder 1987; Katsova 1987). A sample of active main-sequence G stars recently detected in both energy ranges fulfills the same relation as well (Güdel et al. 1993b). In a recent comparison of low-level SXR and microwave luminosities, L_X and L_R, of the coronae of various active stars, Güdel & Benz (1993) report a general relation, which can be represented as

$$L_X/L_R = \kappa \cdot 10^{15.5\pm0.5}\ \text{[Hz]}\,, \qquad (1)$$

over five orders of magnitude, where κ is unity for dMe and dK stars, BY Dra-type binaries, and RS CVn binaries with two (sub)giants. For classical RS CVn binaries, Algol systems, FK Com stars, and post T Tau stars $\kappa \approx 0.17$.

The stellar X-ray emission at wavelengths $\gtrsim 3$Å fits the thermal emission expected from an optically thin plasma with one

or more temperature components around 10^7 K (e.g. Schmitt et al. 1987, 1990); there is an ongoing debate on whether the true emission measure distribution in the coronal plasma is singular, bimodal, or continuous (e.g., Schmitt et al. 1990). VLBI observations and the shallow spectra of dMe and RS CVn microwave emission near 8 GHz are compatible with optically thin gyrosynchrotron radiation of mildly relativistic electrons (e.g., White et al. 1989; Morris et al. 1990; Chiuderi & Franciosini 1993; cf. Güdel 1994 for a summary). As in the case of the SXR/optical-flare ratio, the observed relation between the emissions of thermal and nonthermal particles does not prove a direct causal relation.

The quiet Sun, being an inactive, slow rotator, does not comply with relation (1). This is compatible with the above interpretation of the stellar microwave emission, as there are no indications for relativistic electrons in the low-level (quiet) solar corona. Its microwave radiation is due to thermal free-free and gyroresonance emission. There are, however, nonthermal, mildly relativistic electrons during solar flares as manifest by hard X-ray bremsstrahlung and microwave synchrotron emissions. Do the flare thermal soft X-ray and nonthermal microwave emissions have the same ratio found for the stellar low-level emissions?

The purpose of this paper is to compare solar flare plasma diagnostics with characteristics of the low-level stellar coronal plasma. The different energy ranges conventionally used for solar and stellar X-ray observations do not allow us to directly compare archived observations. Using new GOES calibration procedures developed by Garcia (1993) to determine the temperature T and the volume emission measure EM of the flaring plasma, we transform the observed emission into a lower energy band that can be directly compared with stellar data. The organization of the paper is as follows: In Sect. 2, we present data used for this study, and describe our data analysis; an error analysis is included. In Sect. 3, we present statistical results; Sect. 4 contains a discussion and implications for the role of flares in coronal heating.

2. Observations and analysis

Based on *hard* X-ray observations at energies $\gtrsim 30$ keV, solar flares have been classified into the three types: the most frequent *impulsive* flares originating in compact low-altitude loops with impulsive hard X-ray spikes on time scales of seconds, a total duration of a few minutes and a variable spectral index; *gradual* flares originating from high-altitude sources, with a duration in excess of 10 min, timescales of many minutes, and a monotonically hardening spectral index; and *hot thermal* flares with a relatively soft, thermal X-ray spectrum (see, e.g., Dennis 1988 for a review).

We do not consider hot thermal flares here since they are very rare. Our flare selection comprises three categories related to the impulsive and the gradual flare types: (i) a sample of typical, single *impulsive* flares, identified in Solar Geophysical Data; (ii) a class of very small impulsive *microflares* that have previously been studied in the context of their correlation with microwave events (Fürst et al. 1982); (iii) large *gradual* flare events from a sample investigated by Cliver et al. (1986), supplemented by two similar events taken from Solar Geophysical Data; this sample was split into *pure gradual* events and gradual events that were effectively dominated by *large impulsive* precursors. After searching the available radio and X-ray data, we have found the data of seven impulsive flares, four microflares, four pure gradual events, and five gradual events with impulsive precursors, to be suitable for further analysis. In the following subsections, we describe our data reduction and give an approximate error analysis.

2.1. GOES-2 solar SXR data

The solar soft X-ray observations were obtained by GOES-2 (Geostationary Operational Environmental Satellite) between March 1979 and May 1983. The GOES-2 spacecraft continuously monitored the full Sun in two SXR energy bands, the lower (XL) comprising the interval 1.5–12 keV and the higher (XS) 3–24 keV. The high contrast of flares against background emission at these energies allows sensitive diagnostic measurements. However, the overlap with the bandpasses conventionally used on stellar X-ray satellites (e.g., 0.16–4 keV for *Einstein* IPC, 0.1–2.4 keV for ROSAT PSPC) is small. Figure 1 illustrates optically thin thermal X-ray model spectra calculated by a Raymond-Smith code. Notice that stellar X-ray satellites cover an energy range that is dominated by lines over the temperature range of interest ($1–20 \cdot 10^6$ K). On the other hand, GOES detectors measure in a range of dominant thermal continuum and are therefore very temperature-sensitive; this makes GOES data excellent tools for temperature and emission measure plasma diagnostics. The major task of this study was to carefully calibrate GOES-2 data so that they could be converted to study 'what ROSAT would see if it observed the solar flare'.

The GOES ion-chamber detectors provided electric currents at 0.6 second resolution. The currents were routinely calibrated with a constant calibration factor derived from the wavelength-averaged transfer function. The calibration factor does not take into account the temperature variation during the flares. This rough calibration yields approximate fluxes in energy units, but is inappropriate for the purpose of precise temperature and emission measure diagnostics. Such data were archived on microfilm in the form of lightcurves at 3 second time resolution (Fig. 2), and were made available to us by NOAA. We digitized the flare lightcurves in appropriate time steps; the step was typically 0.5–1 min during the rise phase of impulsive flares, 2–5 min during the decay of impulsive flares or the rise of gradual flares, and up to 30 min during the very slow decay of gradual bursts. For a precise, unbiased integration in the subsequent data analysis we applied spline interpolation to both lightcurves at a constant time resolution corresponding to the smallest time step used to digitize the raw data. The data were then recalibrated by the method outlined below.

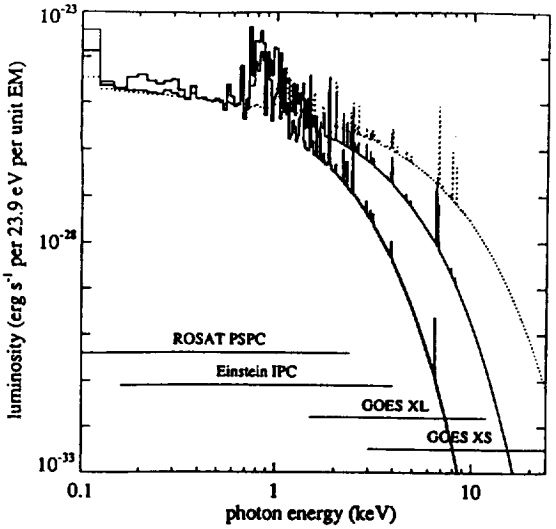

Fig. 1. Soft X-ray spectra calculated by a Raymond-Smith code for a temperature of $5 \cdot 10^6$ K (bold), $10 \cdot 10^6$ K (thin), and $20 \cdot 10^6$ K (dashed). The spectral luminosity is presented as the energy radiated per second by a unit emission measure (cm^{-3}) into a photon energy range of 23.9 eV. The passbands of various X-ray detectors are indicated by bars

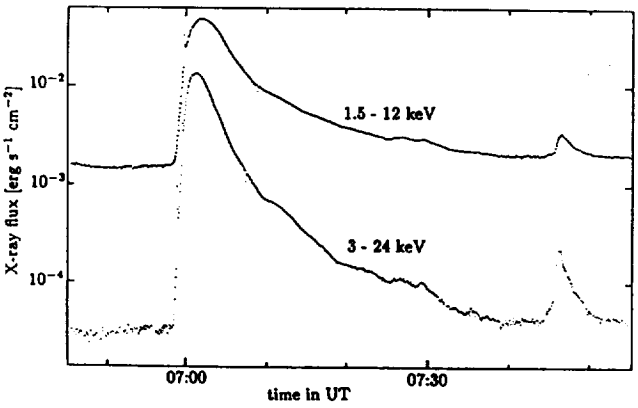

Fig. 2. Example of microfilm-archived GOES-2 solar flare data, observed on 10 August 1981. The two lightcurves show a typical impulsive soft X-ray flare after the rough, temperature-independent calibration. The upper lightcurve represents the 1.5–12 keV (1–8 Å) flux, the lower lightcurve the 3–24 keV (0.5–4 Å) flux. A second, much smaller flare occurred at 07:47 UT. Notice slow modulations in the background prior to the flare onset, and irregularities in the late decay phase

2.2. *X-ray calibration procedures and spectral line models*

Precise temperature-dependent calibration procedures for GOES-2 and error estimates have recently been developed by Garcia (1993) and will be extensively referred to throughout the paper. Details on data acquisition, calibration, and comparisons with other satellite measurements of solar SXR flares are also given by Garcia (1993).

In a first step the rough calibration had to be reversed. We decalibrated the raw microfilm data to obtain the effectively measured ion-chamber currents. In the absence of flaring, GOES data show a gradually varying background level (Fig. 2); this contribution originates from i) various X-ray emitting, nonflaring active regions on the Sun, and ii) from particle contamination in the local environment (bremsstrahlung by magnetospheric electrons with energies $\gtrsim 2$ MeV; Garcia 1993). Obviously, this background cannot be modeled in terms of a unique temperature and emission measure, and needs to be subtracted prior to further data analysis. Since regular flares exceed the background level by one or two orders of magnitude at their peaks, a precise subtraction of the background current is usually not important for high-level emission. However, since we wanted to include very small flares and needed to model the complete lightcurves down to levels close to the background, we estimated the background levels shortly before the onset of the flare and subtracted these constants from the lightcurves. Since the background during flares cannot be monitored separately, background modulations may introduce a small error that may increase with elapsed time. Variations in the background before the onset of the investigated flares occur typically on time scales of several minutes to tens of minutes (Fig. 2). Although the total background level exceeds the fluxes of the smallest observable flares, its variations are not relevant for our microflares, since their duration is shorter than the background modulations. For these events, background-subtracted data were available from Fürst et al. (1982). Thus, our plasma diagnostics involve the flaring plasma only, because we have subtracted the contributions from the quiet solar corona.

In the next step, we estimated the flare electron temperature from the spectral hardness of the two bands, which for our purpose is defined as the ratio between the 1.5–12 keV and the 3–24 keV ion-chamber currents. The ratio is a unique function of temperature and was calculated from model spectra and the GOES-2 transfer function by Garcia (1993). Similarly, the ion-chamber currents $c_0(T)$ induced by a unit emission measure EM_0 at temperature T on the Sun have been tabulated; a recent (1993) version of the emissivity model for an optically thin thermal plasma by Raymond and Smith was used with solar abundances (Garcia 1993). By implication, the total emission measure, EM, pertaining to the observation is found as the ratio between the observed current and $c_0(T)$. We determined the hardness ratios for every time step and used Garcia's tables to find T and EM by linear interpolation.

Having an estimate of the average temperature and the total EM of the flare for each data point, one can, in principle, compute the X-ray luminosity or flux in any passband; this is appropriate as long as the X-ray source can be approximated with an isothermal plasma. The validity of this assumption is discussed in Sect. 2.3 below. We applied the Raymond-Smith code to calculate the flux between selectable passband limits. Figures 3 and 4 show examples of different kinds of flares and their relevant parameters derived from observations. The three lightcurves correspond to the calibrated flux of GOES XL (1.5–12 keV), GOES XS (3–24 keV), and – of primary interest to us – the energy range of the ROSAT PSPC (0.1–2.4 keV).

In the last step, we determined its peak flux and numerically integrated the 0.1–2.4 keV lightcurve in time. Late in the slow

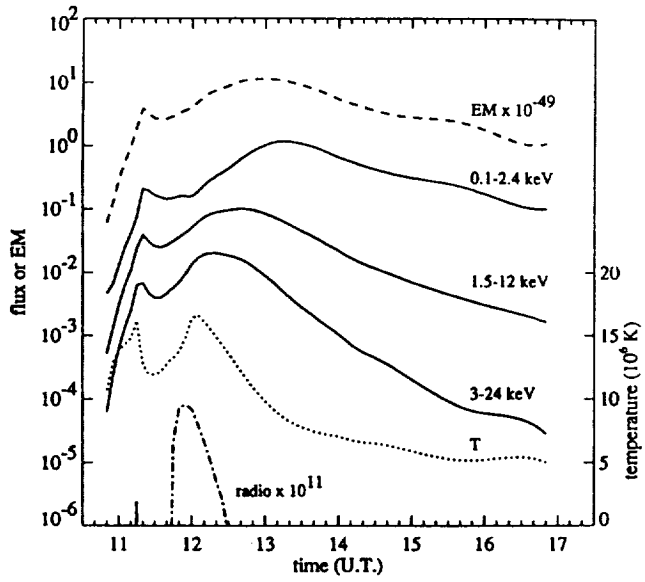

Fig. 3. The calibrated microwave and SXR time profiles of a large *impulsive* solar flare (peak at 11:15 UT, 26 April 1981) and a clearly separable *gradual* flare (12:00–16:00 UT) are shown on a logarithmic scale. The microwave flux (dot-dashed, in solar flux units) was observed at 5 GHz at Sagamore Hill. The observed GOES SXR fluxes (solid curves labeled 1.5–12 keV and 3–24 keV, in erg $s^{-1}cm^{-2}$) have been converted into temperature (T, dotted, linear scale at right) and emission measure (EM, in cm^{-3}, dashed curve, logarithmic scale at left) using tables based on model calculations for a Raymond-Smith type thermal line spectrum and the GOES-2 transfer function (courtesy H. A. Garcia). This is appropriate under the assumption that T and EM are the same for all SXR energy ranges at a given time (isothermal plasma). Integration of the 0.1–2.4 keV portion of the model spectrum yields the total flux to be compared with the ROSAT PSPC stellar data

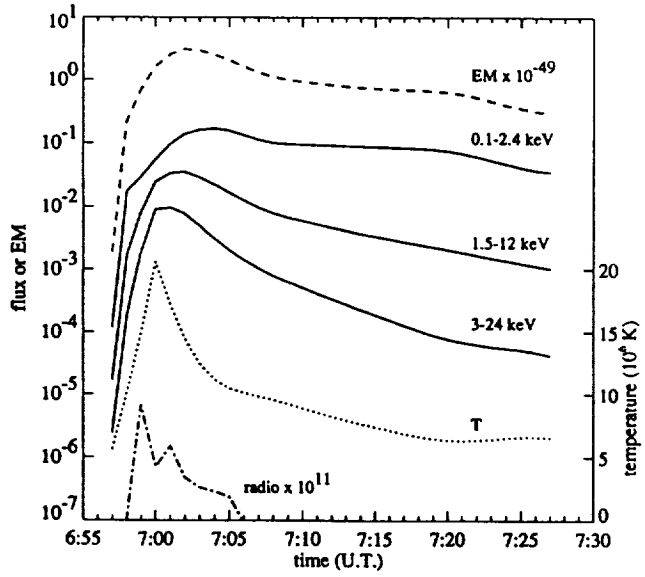

Fig. 4. Similar to Fig. 3 for the single, intermediate-flux, *impulsive* solar flare, observed on 10 August 1981. Note, however, the different time scale! The very small flares or background fluctuations between 07:25–07:30 UT (cf. Fig. 2) were eliminated

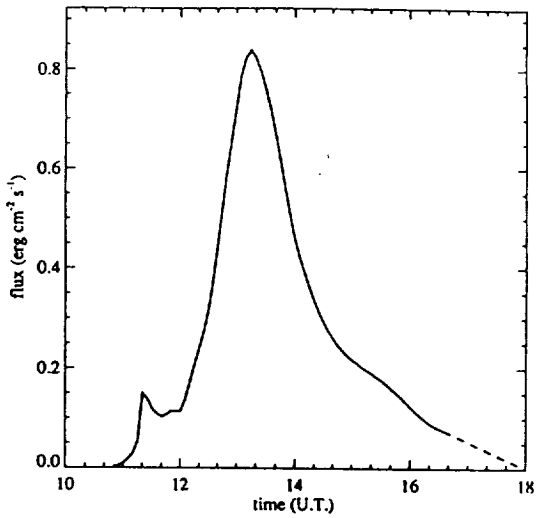

Fig. 5. The flux of the flare in Fig. 3 visible through a passband equivalent to the ROSAT PSPC; the scale is linear, and the end of the event is extrapolated (dashed) for the integration of the total radiated energy during the flare

decay of the flare, when the given GOES fluxes approach the (ill-determined) background, precise evaluation of background-subtracted ion-chamber currents becomes impossible, and hardness ratios can therefore no longer be determined with accuracy (Fig. 2). In most cases the lightcurves, the temperature, and the emission measure monotonically decreased after the flare peak until the 0.1–2.4 keV fluxes reached ~6–15% of the peak flux, while in a few cases the limit was at 15–30%. In some cases, new flares prevented monitoring to later times. We estimated the continuation of the lightcurve beyond that time by eye and added the additional flux. Errors induced by this process are estimated below. As an illustration, Fig. 5 shows a typical lightcurve on a linear scale. The event has an impulsive phase (peak at 11:15 UT) followed by a dominating gradual phase.

We finally defined the equivalent duration d_X of the SXR flare by *twice* the ratio of peak flux to integrated flux of the 0.1–2.4 keV lightcurve.

2.3. *Error estimates for solar SXR data*

Various systematic and statistical errors are affecting individual steps of our X-ray data analysis. A thorough discussion of the effects is beyond the purpose of this paper and is given by Garcia (1993). Here, we briefly mention the relevant errors:

i) The determination of T and EM from GOES data is justified only under the assumption of an isothermal plasma. Inhomogeneous models consisting of several simultaneously emitting sources with different T and EM are beyond the capability of GOES two-channel, full-Sun data. This is similarly true for the stellar X-ray data which, in most cases considered here, have been derived assuming a standard model with a fixed coronal composition in terms of T and EM (usually a two-component plasma, as derived from a few, spectrally modeled sources). Nevertheless, Garcia & Farnik (1992) showed by comparing

PROGNOZ and GOES spacecraft data (with different energy ranges) that the isothermal assumption is a good approximation during most of the solar flare lifetime, with the exception of the initial stage of rapid SXR increase. The effect is less important for the 0.1–2.4 keV data, since that lightcurve reaches its peak only significantly later than the GOES lightcurves (Figs. 3 and 4). Inspection of our lightcurves suggests that a 5–10% error (~ 0.045 dex) is a conservative estimate assuming that only the initial stage of the flare is not accurately represented. It will be clear that most of the errors are not statistical, but systematic and multiplicative. It is therefore practical to represent errors by the logarithm of their factor (abbreviated by *dex*).

ii) Errors introduced by the estimated continuation of the late decay (which cannot be modeled reliably from GOES data, see above) are primarily due to the uncertainty of the time scales of the late decay. In most cases, relative fluxes in that regime were low ($\lesssim$ 10% of the peak flux). We estimate the total error by assuming a time scale uncertainty equal to one half of the duration of the reliably measured lightcurve (approximately corresponding to the reliably measured decay portion of the lightcurve). With this, we find that essentially all uncertainties are between 3 and 15%, most being between 7 and 12%. For convenience, we adopt an average uncertainty of 12% (~ 0.055 dex) for all flares.

iii) Instrumental uncertainties are probably minor for our investigation. Garcia (1993) reports 1σ instrument calibration uncertainties amounting to 3.7% and 2.8% for the XL and XS, respectively. Reading and decalibrating archived fluxes are thus assumed to have an inaccuracy of this order. Systematic SXR measurement errors, to be attributed to shifts in the instrument or the background as compared with other GOES detectors, may amount to 15%, while random variations in the local background are typically 2% in the XL and 8% in the XS. We conservatively adopt the total instrumental measurement uncertainties at $\pm 20\%$ in the following (~ 0.1 dex).

iv) Uncertainties in the model temperatures: Garcia (1993) compared derived temperatures and emission measures for flares observed by different spacecraft. Based on his findings, we conservatively assume a temperature error in his tables for the current ratios of $\pm 1 \cdot 10^6$ K, which may introduce typical errors of up to $\sim$ 20% around $1 \cdot 10^6$ K (less at higher temperatures) in the emission measures. Furthermore, systematic deviations exist in the determination of the emission measures between different spacecraft, probably due to the application of different plasma model codes used for the modeling. We adopt a combined uncertainty in the EM determination of 30% here (~ 0.15 dex); since the 0.1–2.4 keV flux basically scales with EM, this is also the adopted error in the flux measurements. The accuracy of the Raymond-Smith model calculations performed by us based on T and EM is difficult to quantify; comparisons between recent codes indicate that an error estimate of 10% ($\sim$ 0.046 dex) is appropriate.

It is somewhat tentative to provide total error estimates for our data given that the results are affected by various systematic and statistical, instrumental, computational, magnetospheric, and solar influences that are not well understood and are in part variable. Unknown sources of error may exist as well (e.g., inhomogeneities in the X-ray source, concurrent flare contributions, or background contamination during the decaying flare). The most significant errors are not statistical. We propose to consider a worst case error analysis here, with all errors being multiplicative in the same sense. *Peak* fluxes are principally affected by errors (iii) and (iv), while all errors (i)–(iv) contribute to the *integrated* fluxes. With the above estimates, we find a conservative estimate of the combined errors in the solar SXR data of 0.3 dex (factor of 2) and 0.4 dex (factor of 2.5) for peak and integrated fluxes, respectively (the statistical mean square error would be $\sim$0.2 dex or a factor of 1.6 in both cases). While this at first sight appears large, it appropriately reflects basic uncertainties and is in fact moderate compared with the range of SXR luminosities covered in Figs. 6 and 7 and compared with the scatter in the data.

2.4. *The solar microwave data and their errors*

Radio data for solar flares were obtained from Solar Geophysical Data, the Bern Observatory Reports, Fürst et al. (1982), and Cliver et al. (1986). Since stellar data were obtained between 5 and 8.5 GHz, we searched for solar observations at frequencies in that range. Usually, 8–9 GHz data were available. In some cases the flux had to be interpolated using different data sets obtained at several frequencies between 5 and 20 GHz. The accuracy of the interpolation depends on the spectral shape, but variations between 5 and 20 GHz suggest that errors introduced here are less than 0.1 dex.

The accuracy of the instrumental calibration is difficult to estimate, but based on comparisons of similar flare measurements from different observatories we assume that errors up to a few tens of percent are possible. The integrated fluxes were calculated from lightcurves on a linear flux scale, and are subject to uncertainties in the slow decay phase similar to the SXR flares. In one case, no lightcurve was available; we estimated the integrated flux as the product of the FWHM time and the peak flux, as given in Cliver et al. (1986). We tested this approximation for several flares for which we had FWHM/peak flux data and lightcurves available; the deviations between the two results always agreed within $10\pm5\%$. In summary, to cover all known and possible systematic effects, we conservatively put error bars of 0.2 dex (factor of 1.6) and 0.3 dex (factor of 2) for all radio peak and integrated fluxes, respectively. We mention here that for two flares of the gradual type with impulsive precursors only peak radio fluxes were available from the literature. These events will thus not appear in the statistics on average flare fluxes.

2.5. *Stellar X-ray data*

Most stellar SXR data used in this investigation are from the surveys obtained by *Einstein* and ROSAT; the full list of references used for Fig. 6 has been given in Güdel & Benz (1993). Data on M-dwarfs are from Güdel et al. (1993a) who extracted X-ray luminosities from the ROSAT All-Sky Survey and ob-

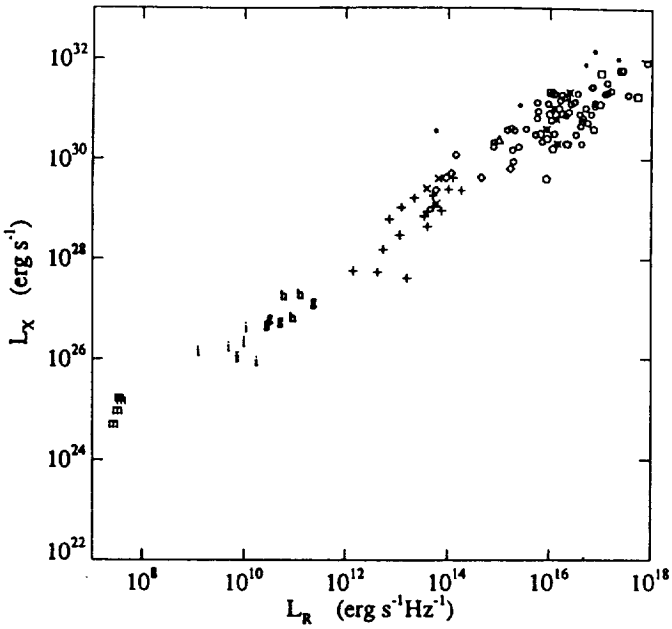

Fig. 6. Comparison of soft X-ray and microwave luminosities of solar flares and active corona stars of different classes. The *time averaged* flux values are used for the flares. The stellar data have been presented previously by Güdel and Benz (1993), where the references are listed. Key to the symbols: *m* solar microflare; *i* intermediate impulsive solar flare; *h* gradual solar flare with dominating large impulsive phase; *g* pure gradual solar flare; + dM(e) stars; × dK(e) stars; ◇ BY Dra binaries; ○ RS CVn binaries; ○ RS CVn binaries with two giants; △ AB Dor; * Algol-type binaries; □ FK Com stars; (pentagon) post-T Tau stars

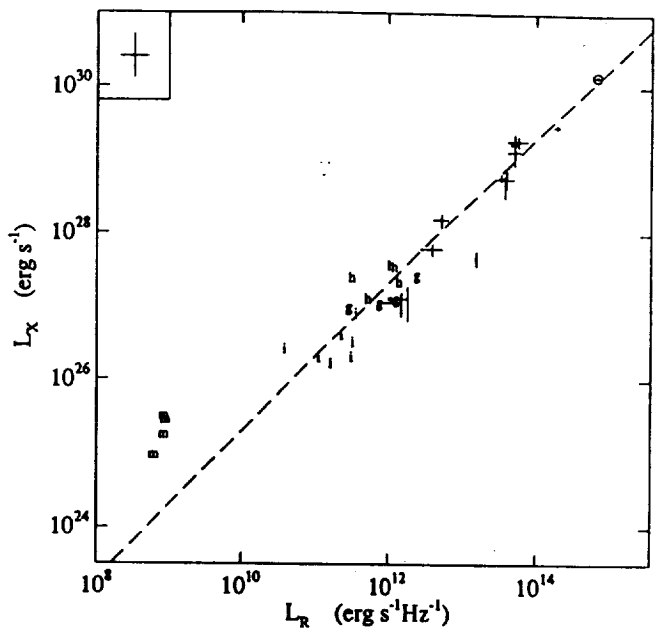

Fig. 7. Detailed comparison of *peak* solar flare luminosities with dMe stars (from Güdel et al. 1993a) in SXR and microwave emissions. The estimated error bars for the solar observations are given in the top left corner. The dMe stars are represented with error bars, the letters refer to the solar flares (for the key see Fig. 6). The dashed line is a fitting line with slope 1 to the dMe stars. A long duration flare on the M dwarf EQ Peg B is shown by a circle around its error bars. Its microwave emission has been interpreted by the gyrosynchrotron mechanism (Kundu et al. 1988)

tained mostly near-simultaneous radio observations at 4.9 and 8.5 GHz with the VLA. The SXR passbands of ROSAT and *Einstein* are different. At 10^7 K the ROSAT PSPC flux is, based on theoretical model spectra, expected to be about 13% higher. This difference is well within the estimated errors from other sources, and also significantly smaller than the usual stellar coronal variability; while we compare in Fig. 6 stellar data both from the *Einstein* IPC and the ROSAT PSPC, we will later concentrate on an X-ray data set of M dwarfs obtained by ROSAT only (Fig. 7); thus, for the purpose of our investigation, the possible but small systematic deviation between *Einstein* and ROSAT data is irrelevant and will be neglected. We will not consider intrinsic variability in the stellar X-ray (and radio) luminosities, since the data set on M dwarfs was obtained simultaneously in X-rays and microwaves (Güdel et al. 1993a).

We have subtracted the SXR background radiation from the solar data, including contributions from the non-flaring, quiet Sun (Sect. 2.2). Stellar coronae may possess a low temperature background level as well (a possible interpretation involves the lower temperature component in two-temperature X-ray fits; see Lemen et al. 1989), but the emission measure pertaining to the steady stellar X-ray radiation is clearly dominated by the usually much hotter ($1–2 \cdot 10^7$ K) stellar plasma component that is not present on the quiet Sun. Furthermore, the true emission measure distribution of stellar coronae is still under debate, and may be determined unambiguously only with spectrally resolving X-ray detectors. It may well be that the bimodal distribution found on many stars is induced by detector characteristics, and that the underlying distribution is in fact continuous (e.g., Majer et al. 1986; Schmitt et al. 1987). We are thus presently not in the position to define and separate out any possible quiet plasma component, and will not consider this question for our analysis.

The relevant errors in the stellar SXR luminosities result mainly from *counting statistics, uncertainties in the temperature model, in the emissivity model, and in the interstellar absorption*. The error in distance cancels when the SXR luminosity is compared to the microwave luminosity. Variation in the (mostly unknown) coronal composition in terms of dominating temperatures, typically between 2 and $20 \cdot 10^6$ K, introduces a (systematic, but unknown) uncertainty of about 0.12 dex. As for solar data, we estimate errors in the emissivity model at 0.045 dex. The error introduced by the estimated interstellar absorption is negligible for nearby dMe stars, but increases with distance. We thus adopt a total systematic error of about 0.18 dex (factor of 1.5), beside the statistical error due to counting statistics. The plot of stellar observations in Fig. 7 only shows the 1σ error bars from the counting statistics.

2.6. Stellar microwave data

The error in the stellar microwave data is mostly due to *measurement noise* and the *unknown optical depth* of the coronal plasma to microwaves. While we can argue that 5–8 GHz emission from active but nonflaring stars is usually optically thin, the precise value of the optical depth τ is unknown and certainly varies in different sources. If τ exceeded unity, the emission would saturate and the correlation with SXR would fail as is clearly manifest in one of the solar events (cf. Sect. 3). We take the small scatter of the stellar data around the fitting line as an indication that the finite τ among stellar sources within the frequency range considered here is *not* the dominant source of error in M and K-dwarfs. In Fig. 7 the noise contributions to the error for each observation is shown.

2.7. Comparison between solar and stellar data

The temperature of the SXR emitting plasma cannot be derived from the ROSAT survey for the sources considered here. To estimate fluxes (in erg $s^{-1}cm^{-2}$) from the measured count rates, it is common to apply a standard conversion factor, e.g. $6{\cdot}10^{-12}$ erg cm^{-2} per count for ROSAT. This conversion factor is appropriate for average active coronae that are generally described in terms of two components with different temperatures and emission measures. Schmitt et al. (1990) find, in the average on dMe stars, two components at temperatures $\log T_1 = 6.4$ and $\log T_2 = 7.2$, with $EM_2/EM_1 \approx 3 \pm 1$. Our results derived from GOES are, however, based on a single temperature by definition. To compare solar flare data with stellar data from the ROSAT All-Sky Survey, we derived theoretical conversion factors from count rates to flux for single temperature plasmas, using Raymond-Smith models as implemented in the IRAF/PROS software package. If the solar flares were observed by a ROSAT PSPC-type instrument, and the same standard conversion factor were applied, the fluxes would be 72% of the fluxes derived from GOES by the above procedures. To compare solar and stellar data, the solar flare fluxes were thus multiplied by 0.72 after calibration.

Solar flare microwaves show considerable variation in the 1–20 GHz range. At low frequencies, the sources are optically thick and the flux increases with frequency according to a power-law of index 0–10. Beyond some spectral peak, the sources become optically thin and decrease with a power-law index of about -1 to -5. Gradual solar flares tend to be optically thin at 5–10 GHz; the turnover frequencies are mostly smaller than 5 GHz and often less than 2 GHz (Cliver et al. 1986), apparently very similar to the quiescent emission of many stellar sources. On the other hand, turnover frequencies of impulsive flares range more typically between 10 and 20 GHz, thus making 5–10 GHz emission optically thick. The class of impulsive solar flares therefore requires a systematic correction when compared to stars. We have estimated the effect from the spectra of the investigated flares. Using the high-frequency slope to estimate the flux density at 8 GHz as if the source were optically thin, the values have to be increased by 0.06 to 0.37 dex (with the exception of an event to be discussed below). There is no information on the spectrum of the microflares, which were observed, however, at the relatively high frequency of 10.69 GHz. We have not attempted to correct for the effect of finite optical thickness neither in solar nor stellar microwave luminosities.

2.8. Summary of the error analysis

We have discussed estimated errors of solar and stellar data in Sects. 2.2–7 and briefly summarize the relevant numbers. i) Statistical errors in the measurements of solar X-ray and microwave fluxes are small and can be fully neglected here. ii) Statistical errors in the stellar observations are shown explicitly in Fig. 7 for dMe star observations. They are typically of the order of 0.1 dex. iii) Systematic but unknown errors in the solar X-ray observations amount to 0.3 dex and 0.4 dex for peak and integrated values, respectively. iv) Systematic errors in the solar microwave observations are estimated to be 0.2 dex and 0.3 dex for peak and integrated values, respectively. v) Additional sources of error in stellar X-ray observations are estimated at 0.18 dex, mainly due to the unknown composition of the stellar plasma. vi) Systematic errors in stellar radio observations due to optical depth do not seem to dominate the results, and are not considered here. vii) To compare solar and stellar SXR data obtained under different model assumptions, solar SXR data have to be reduced to 72% of the computed values. This effect has been fully corrected in Figs. 5, 6, and 7 and in our statistical analysis. viii) To compare solar *impulsive* microwave flares with stellar microwave data, the radio flare fluxes have to be increased by a considerable, but highly variable factor to compensate for optical thickness; microwave spectral characteristics of *gradual* flares and stellar emissions are relatively similar and do probably not require a significant adjustment due to the optical depth.

3. Results

Figures 3 and 4 show typical characteristics of solar flares well-known for both the gradual and impulsive types. The microwaves peak first, followed by maximum temperature of the flare plasma of some $1\text{–}3{\cdot}10^7$ K. As the plasma cools but the emission measure still rises, the peak of the soft X-rays is delayed; the delay is larger for the lower energy bands. Notice that the higher energy fluxes strongly depend on the evolution of the temperature, while the lower energy, 0.1–2.4 keV lightcurve closely resembles the evolution of the emission measure. This observation reflects the temperature sensitivity of the upper energy band and (relative) insensitivity of the lower energy band, ideal for flare diagnostics (Sect. 2.1). The microwaves peak approximately at the time of maximum temperature increase. Given that the microwave lightcurve closely correlates with the hard X-ray time history (particularly in impulsive flares; e.g., review by Dennis 1988), this observation is in agreement with the previously reported correlation between the SXR lightcurve and the integral of the hard X-ray time profile (Neupert 1968). It has been taken as evidence that the thermal source emitting the

SXRs is in part produced by high-energy electrons (see Dennis 1988 for a discussion).

Figure 6 presents average luminosities of solar flares and low-level coronal emissions of stars. The derived solar flare 0.1–2.4 keV X-ray fluxes and the microwave flux densities were integrated in time and divided by the equivalent duration, d_X, of the SXR emission. Solar and stellar values correlate over many orders of magnitude. The *overall* correlation is not linear as given in Eq. (1), i.e. the slope differs from unity in the log–log plot and amounts to 0.73 ± 0.03 (number of entries N = 102, correlation coefficient for L_X versus L_R: $R = 0.91$). Note, however, that the relation is approximately linear within the M and K dwarfs and within the RS CVn classes (Güdel et al. 1993a; Güdel 1992; Drake et al. 1992). The solar flares connect smoothly to the active star coronae in the L_X/L_R-plot.

The slope for the solar flares is smaller than unity, but this is a result mainly produced by the microflares. All four microflares have been observed on the same day with a narrow microwave beam (100 m telescope in Effelsberg) which may not have been centered on the source. A comparison with full Sun telescopes has shown that this may account for a factor of 3 at most (Fürst et al. 1982). If, on the other hand, the relative weakness of microwaves in microflares is real, the non-linearity means that the microwave productivity increases with increasing flare size, or, from the microwave point of view, the X-ray luminosity is relatively higher in small flares. Microflares possibly involve acceleration and trapping at low altitudes (Benz et al. 1981). This would lead to small particle lifetimes and naturally explain the weak microwave emission and that they deviate most from the fitting line to the dMe coronae in Fig. 7.

Apart from the microflares, the solar flare observations are compatible with a *linear* correlation, $L_R \propto L_X$. The impulsive flare ('i' in Fig. 6) with the weakest radio luminosity had its spectral peak beyond 35 GHz (Bern Observatory Report). Its 8 GHz flux shown in Fig. 6 was therefore reduced by optical thickness exceeding unity and the correction for this effect would be of the order of 1 dex. Excluding this exceptional event and the microflares, we find a least-squares linear regression in the log-log plot with a slope of 0.91±0.13 (N = 13, R = 0.85). Furthermore, the observed scatter of about 0.26 dex in L_X around the fitting line favorably agrees with the estimated total error, thus indicating that the observations are compatible with a linear correlation. Several individual solar flares fall within the error ranges of the linear relation pertaining to the M dwarfs , although the average solar flare (excluding the microflares) X-ray/microwave ratio exceeds the value of M dwarfs by a factor of 4.7 (0.67 dex).

The solar microwave flares are considerably shorter than the enhanced SXR emission (by a factor of about 5; Figs. 3 and 4). Thus, the use of flare average values for a comparison with stellar low-level radiation seems to be appropriate. Nevertheless, we replaced the average flare values by the peak fluxes to further investigate the correlation. The results are compared in Fig. 7 with the low-level emissions of dMe stars that have been measured strictly simultaneously (Güdel et al. 1993a) and have a linear L_X-L_R relation. The solar flare peak data have the same L_X/L_R ratio except for the microflares, which deviate by an order of magnitude from the fit to the stellar data. The least-squares linear regression fit to the logarithmic data in Fig. 7 (solar and stellar flares and stellar coronae, but excluding the microflares) has a slope of 1.02±0.17, clearly compatible with a proportionality $L_R \propto L_X$ (N = 16, R = 0.78). The statistical scatter in L_X around the linear fit amounts to 0.31 dex, again compatible with the estimated total error (Sect. 2.3).

We are aware of only one simultaneous microwave and X-ray observation of a *stellar* flare detected in both regimes whose radio emission is compatible with the gyrosynchrotron process. This extremely long-duration, only weakly polarized stellar flare on EQ Peg was observed by Kundu et al. (1988) with EXOSAT and the VLA and is found to fit well into the ratio observed for the low-level stellar emissions (Fig. 7). The approximate peak value is shown, as the time histories of both radiations are only partially known. It is interesting to note that the microwave decay time seems to be longer than the SXR decay time, opposite to solar flares. Note that highly polarized microwave flare emission as often observed on dMe stars is unlikely to originate from the synchrotron mechanism and is therefore not suitable for this comparison.

4. Discussion

We propose to discuss the correlation found in Figs. 6 and 7 in terms of a process that both heats and accelerates by constant fractions. This naturally leads to a linear relation between L_X and L_R with a slightly variable ratio similar to Eq. (1). The ratio is given by

$$L_X/L_R \approx 1.06 \cdot 10^{22}\, B^{-2.48} \frac{b}{a} \frac{1}{\tau_0(\alpha+1)} \quad [\mathrm{Hz}]\,, \qquad (2)$$

(Güdel & Benz 1993) where B is the magnetic field in the microwave source in units of Gauss, a (< 1) is the efficiency of the coronal heating process to accelerate particles, b is the fraction of coronal energy lost by radiation into the observed X-ray band (PSPC: 0.1–2.4 keV), τ_0 is the average lifetime in seconds of energetic electrons at the low-energy cutoff (normalized to be 10 keV), and $\alpha(> -1)$ is the power-law exponent of the lifetime vs. energy. It has been assumed that the density of energetic electrons obeys a power-law distribution decreasing in energy with a power of -3. This is compatible with stellar microwave spectra and measurements of hard X-rays during peaks of solar impulsive flares, and peaks and decays of solar gradual flares (cf. Güdel 1994). The gyrosynchrotron emissivity given by Dulk & Marsh (1982) was used.

When considered separately, each class of objects (including regular flares, dMe, dK, and RS CVn coronae) seems to be compatible with a linear relation between X-rays and microwaves. Different classes of objects, however, have a different average L_X/L_R ratio.

If the integrated and averaged solar flare microwave luminosity were used as an estimate of the stellar energy input into the corona by an acceleration process as efficient as in solar flares, the predicted stellar (dMe) thermal SXR emission would

be larger than observed by a factor of 4.7. Some fraction of this difference may be caused by optical depth effects of the solar flare microwaves. Other possible causes include higher densities and shorter particle lifetimes in the solar corona due to lower-lying, more compact loops compared to active, hotter stellar coronae. In particular, this is plausible for the very small microflares. Since active stars are likely to have stronger magnetic fields and larger spots than the Sun, loops in stellar coronae may be larger and offer better traps for relativistic particles, allowing them to lose a larger portion of their energy into gyrosynchrotron radiation before they collide with other particles. The long timescales of the radio flare on EQ Peg may be taken as evidence for this. It would also explain the tendency of stellar coronae to be microwave-rich as compared to solar flares.

We note that the agreement between solar flares and stellar coronae is much better if peak flare values are used. The L_X/L_R ratios for solar flare peaks are lower as compared to integrated values, since the duration of the solar microwave flares is systematically shorter than the duration of the accompanying X-ray flares. This factor (of about 5) coincides with the factor by which solar flares are microwave-poor compared to stellar coronae.

We should caution that many of the errors are *systematic* and may go into the same direction. The average deviation of the L_R and L_X values from a slope=1 line in Fig. 7 is less than the sum of the total errors adopted for solar flare observations and the systematic errors possibly affecting stellar observations. The possibility of an identical L_R/L_X ratio even for integrated solar flare values and stellar coronae cannot be excluded.

It is interesting to note that gradual solar flares are microwave-rich by an order of magnitude compared to impulsive solar flares, if *hard* X-rays ($\gtrsim$ 30 keV) are used as the reference (Cliver et al. 1986). For example, such a difference arises if the lifetime of the microwave emitting particles were longer in the gradual flares. However, using *soft* X-rays as the reference, Figs. 6 and 7 show that the L_X/L_R ratios of impulsive and gradual flares are similar. A possible explanation is a lower SXR productivity (parameterized by the factor b) of gradual flares, where other losses, such as conduction and adiabatic expansion, are expected to be relatively severe. It remains unclear whether b changes enough to also explain the large deviation of microflares. The fraction of input energy radiated in SXR has been estimated to vary only from 0.3 to 0.5 from quiet regions to active regions of the solar corona by Withbroe & Noyes (1977). This cannot explain the trend of the microflares to be X-ray-rich. Thus we expect that other parameters play a similar or larger role.

Whatever the reason for the relatively low average microwave luminosity of solar flares, we find that the larger flares, rather than the microflares, have similar L_R/L_X ratios as stellar coronae. The fact that the stellar flare produced the same L_X/L_R ratio as the low-level emission is further evidence that the processes at work in coronal heating are related or similar to the flare mechanism. The stellar flares having the L_X/L_R ratio of stellar coronae strongly suggest that the deviation of the solar flares is characteristic to the Sun rather than to flares in general. It is surprising that even the conditions for particle acceleration and trapping may be similar in flares and quiescent coronae; at least the parameters controlling the two processes apparently multiply to a similar ratio in Eq. (2) (as indicated by the correlation in Figs. 6 and 7).

These observations suggest that the dominating heating process of active stellar coronae has some of the characteristics of flares: it accelerates electrons to similar energies with similar efficiency, and the particles live long enough to produce a comparable ratio of gyrosynchrotron emission.

Acknowledgements. We thank Howard Garcia (NIST) and Eric Kihn (NOAA) for invaluable help on data processing and interpretation of GOES X-ray data. Steve Drake provided us with a recent version of the Raymond-Smith code for thermal plasmas. This work was supported by Swiss National Science Foundation grants 8220-033360 and 20-34045.92, NASA grants NAG5-1887, through the University of Colorado, and W17,772, through NIST.

References

Ambruster C.W., Sciortino S., Golub L., 1987, ApJS 65, 273
Benz A.O., Fürst E., Hirth W., Perrenoud M.R., 1981, Nature 291, 239
Bookbinder J.A., 1987, in: Havnes O., Pettersen B.R., Schmitt J.H.M.M., Solheim J.E. (eds) Activity in Cool Star Envelopes, Kluwer, Dordrecht, p. 257
Chiuderi-Drago F., Franciosini E., 1993, ApJ, in press
Cliver E.W., Dennis B.R., Kiplinger A.L., Kane S.R., Neidig D.F., Sheeley N.R.Jr., Koomen M.J., 1986, ApJ 305, 920
Dempsey R.C., Linsky J.L., Fleming T.A., Schmitt J.H.M.M., 1993, ApJS 86, 599
Dennis B.R., 1988, Solar Phys 118, 49
Doyle J.G. Butler C.J., 1985, Nature 313, 378
Drake S.A., Simon T., Linsky J.L., 1989, ApJ 71, 905
Drake S.A., Simon T., Linsky J.L., 1992, ApJ 82, 311
Dulk G.A., Marsh K.A., 1982, ApJ 259, 350
Fürst E., Benz A.O., Hirth W., 1982, A&A 107, 178
Garcia H.A., 1993, submitted to Solar Phys.
Garcia H.A., Farnik F., 1992, Solar Phys. 141, 127
Güdel M., 1992, A&A 264, L31
Güdel M., 1994, ApJS, in press
Güdel M., Benz A.O., 1993, ApJ 405, L63
Güdel M., Schmitt J.H.M.M., Benz A.O., 1993b, BAAS 25, 874
Güdel M., Schmitt J.H.M.M., Bookbinder J.A., Fleming T., 1993a, ApJ, in press
Katsova M.M., 1987, in: Havnes O., Pettersen B.R., Schmitt J.H.M.M., Solheim J.E. (eds) Activity in Cool Star Envelopes, Kluwer, Dordrecht, p. 245
Kundu M.R., Pallavicini R., White S.M., Jackson P.D., 1988, A&A 195, 15
Lemen J.R., Mewe R., Schrijver C.J., Fludra A., 1989, ApJ 341, 474
Majer P., Schmitt J.H.M.M., Golub L., Harnden F.R.Jr., Rosner R., 1986, ApJ 300, 360
Morris D.H., Mutel R.L., Su B., 1990, ApJ 362, 299
Neupert W.M., 1968, ApJ 153, L59
Schmitt J.H.M.M., Pallavicini R., Monsignori-Fossi B.C., Harnden F.R.Jr., 1987, A&A, 179, 193
Schmitt J.H.M.M., Collura A., Sciortino S., Vaiana G.S., Harnden F.R.Jr., Rosner R., 1990, ApJ 365, 704

Skumanich A., 1985, Aust. J. Phys. 38, 971
White S.M., Kundu M.R., Jackson P.D., 1989, A&A 225, 112
Whitehouse D.R., 1985, A&A 145, 449
Withbroe G.L., Noyes R.W., 1977, ARA&A 15, 363